Article

Discovery Medicine 2025; 37(203): 2966–2977
https://doi.org/10.24976/Discov.Med.202537203.248

Inhibition of eIF2α Phosphorylation Enhances the Sensitivity of Renal Cell Carcinoma Cells to Sorafenib-Induced Ferroptosis

Lihang Yu[1], Chuanchuan Zhan[1], Jiajun Yan[1], Ke Gao[1], Chong Shen[1], Yu Ren[1,*]

[1]Department of Urology, Shaoxing People's Hospital, 312000 Shaoxing, Zhejiang, China
*Correspondence: 13505755686@163.com (Yu Ren)
Submitted: 19 September 2025 Revised: 6 November 2025 Accepted: 11 November 2025 Published: 20 December 2025

Background: Sorafenib exerts its anti-tumor effects partly by inducing ferroptosis. However, the upstream regulatory mechanisms governing this process, particularly the role of eukaryotic translation initiation factor 2α (eIF2α) phosphorylation, remain largely unclear in renal cell carcinoma (RCC). Therefore, this study aimed to investigate the role and regulatory mechanism of eIF2α phosphorylation in sorafenib-induced ferroptosis in RCC.

Methods: To determine the optimal concentration, RCC cells were treated with sorafenib at doses of 0, 2.5, 5, 10, and 20 µM. Subsequently, sorafenib (10 µM) was administered to RCC cells either alone or in combination with ferrostatin-1 (Fer-1, 5 µM) or Isrib (200 nM). Lipid peroxidation, cell viability, apoptosis, and intracellular Fe^{2+} levels were assessed. *In vivo* BALB/c nude mice bearing orthotopic RCC tumors received intraperitoneal injections of sorafenib (20 mg/kg) or Isrib (2.5 mg/kg). Tumor volume and survival were recorded, while ferroptosis-related proteins, p-EIF2α/EIF2α ratios, and tumor lipid peroxidation (4-hydroxynonenal, 4-HNE) were evaluated.

Results: Sorafenib significantly reduced cell viability, increased apoptosis and lipid peroxidation, downregulated glutathione peroxidase 4 (GPX4), and elevated Fe^{2+} levels and acyl-CoA synthetase long-chain family member 4 (ACSL4) expression ($p < 0.05$). Fer-1 reduced the effects of sorafenib ($p < 0.05$), whereas Isrib enhanced them ($p < 0.05$). Fer-1 further promoted sorafenib-induced phosphorylation of eIF2α ($p < 0.01$), while Isrib inhibited this regulation ($p < 0.001$). *In vitro* experiments also confirmed that inhibition of eIF2α phosphorylation enhanced the anti-tumor effect of sorafenib ($p < 0.05$).

Conclusion: This study reveals eIF2α phosphorylation as a pivotal regulator of sorafenib-induced ferroptosis in RCC. Specifically, inhibition of eIF2α phosphorylation enhances sorafenib-mediated ferroptosis by modulating key ferroptosis-associated proteins and lipid peroxidation, thereby improving sorafenib sensitivity and anti-tumor efficacy in RCC. Targeting eIF2α phosphorylation thus represents a potential strategy to optimize sorafenib-based RCC therapy, based on these new insights into the drug's molecular mechanism of action.

Keywords: renal cell carcinoma; ferroptosis; sorafenib; eukaryotic translation initiation factor 2α phosphorylation; Isrib

Introduction

A steady rise has been observed in the global incidence of kidney cancer in recent years, accounting for approximately 2.2% of new cancer cases and 1.8% of cancer-related deaths worldwide [1]. Among these, renal cell carcinoma (RCC), which originates from the renal epithelium, is the predominant subtype of kidney cancer, representing nearly 90% of all renal cell malignancies [2]. Although RCC commonly occurs within the genitourinary system, most cases are diagnosed at a locally advanced or metastatic stage. At present, available treatments for RCC include radical nephrectomy and partial nephrectomy, along with adjuvant and targeted therapies for patients with metastatic RCC [3]. Sorafenib has been approved for the treatment of RCC for 18 years and was the first targeted therapeutic agent approved for metastatic RCC [4]. Despite providing significant survival benefits for patients with unresectable RCC, the emergence of drug resistance has become a major challenge in sorafenib therapy [5,6]. Therefore, exploring novel therapeutic targets and strategies to enhance tumor sensitivity to sorafenib remains an urgent priority for the effective management of advanced RCC.

Sorafenib has been reported to induce ferroptosis in tumor cells, and ferroptosis has also been implicated in the mechanisms underlying sorafenib resistance [7]. Ferroptosis, a recently characterized form of iron-dependent, non-apoptotic cell death, is primarily associated with the accumulation of intracellular Fe^{2+} and lipid reactive oxygen species (ROS) [8]. Numerous studies have shown that inducing ferroptosis can reverse sorafenib resistance in hepatocellular carcinoma cells [7]. Notably, ferroptosis-related regulators are dysregulated in RCC, suggesting that targeting ferroptosis represents a potential therapeutic approach

for RCC [9]. Moreover, the regulation of ferroptosis-related signaling pathways has been shown to improve the sensitivity of RCC to radiotherapy or chemotherapy [10]. Collectively, these findings suggest that regulation of ferroptosis-related pathways may increase RCC cell sensitivity to sorafenib.

Recent evidence indicates that the therapeutic efficacy of sorafenib is closely related to the phosphorylation level of eukaryotic translation initiation factor 2α (eIF2α) [11]. eIF2α, a regulatory subunit of eIF2, occupies a central position in translation regulation and can be functionally inactivated through phosphorylation. Phosphorylation of eIF2α leads to a reduction in global protein synthesis [12]. In addition to its role in translational control, eIF2α phosphorylation acts as a core component of the integrated stress response, coordinating cellular adaptive transcriptional reprogramming that is essential for cell survival under stress conditions [13]. Notably, endoplasmic reticulum stress has been shown to directly contribute to sorafenib resistance in liver cancer through specific molecular pathways, such as the miR-188-5p/heterogeneous nuclear ribonucleoprotein A2/B1 (hnRNPA2B1)/pyruvate kinase M2 (PKM2) axis [14]. Additionally, phosphorylation of eIF2α promotes activation of activating transcription factor-4 (ATF4), which in turn upregulates solute carrier family 7 member 11 (SLC7A11) [15]. SLC7A11 is a key ferroptosis-related gene that suppresses ferroptosis to promote tumor growth [16] and simultaneously promotes resistance to tumor cells from chemotherapeutic agents [17]. Therefore, it is reasonable to hypothesize that eIF2α phosphorylation may promote RCC cell resistance to sorafenib by inhibiting ferroptosis.

Materials and Methods

Cell Culture

Human RCC cell lines 769-P (AW-CH0007) and 786-O (AW-CH0008) were cultured in Roswell Park Memorial Institute 1640 (RPMI-1640) medium (AW-002, AnWei-sci, Shanghai, China) supplemented with 10% fetal bovine serum (FBS, AW-001, AnWei-sci, Shanghai, China). Cells were maintained at 37 °C in a humidified incubator with 5% CO_2 (Forma Steri-Cult, Thermo Fisher, USA). All cell lines were obtained from AnWei-sci (Shanghai, China). Short tandem repeat (STR) profiling confirmed cell line authenticity, and all were tested negative for mycoplasma contamination.

Cell Grouping

The optimal concentration of sorafenib required to inhibit cell viability was first determined. 769-P and 786-O cells were exposed to varying concentrations of sorafenib (0, 2.5, 5, 10, and 20 µM). After 48 h of incubation, cell viability was assessed using the Cell Counting Kit-8 (CCK-8). Subsequently, the experiment was divided into two parts. In the first part, cells were divided into three groups: (1) Control group: normal culture conditions; (2) Sorafenib group: treated with 10 µM sorafenib (HY-10201, MedChemExpress, China) for 24 h; and (3) Sorafenib + Ferrostatin-1 group: pre-treated with 5 µM Fer-1 (Fer-1, HY-100579, MedChemExpress, Shanghai, China), a ferroptosis inhibitor [18] for 1 h, followed by 10 µM sorafenib treatment for 24 h.

In the second part, cells were also divided into three groups: (1) Control group: normal culture conditions; (2) Sorafenib group: treated with 10 µM sorafenib for 24 h; and (3) Sorafenib + Isrib group: co-treated with 10 µM sorafenib and 200 nM Isrib [19] (HY-12495, MedChemExpress, Shanghai, China), an inhibitor of eIF2α phosphorylation, for 24 h.

Cell Viability

RCC cell viability was assessed using the CCK-8 assay (D002-1, Research-bio, Shanghai, China). Briefly, 2×10^3 treated RCC cells were seeded in 96-well plates (FCP962, Beyotime, Shanghai, China) and cultured overnight. Subsequently, 20 µL of CCK-8 reagent was added to each well and incubated for 2 h. Optical density (OD) at 450 nm was measured using an microplate reader (1681135, Bio-Rad Laboratories, Shanghai, China). Relative cell viability was determined using the following formula:

$$\text{Relative cell viability (\%)} = (OD_{Experimental} - OD_{Blank}) / (OD_{Control} - OD_{Blank}) \times 100$$

Apoptosis Assay

Apoptosis was evaluated using an Annexin V-FITC Apoptosis Detection Kit (A432, Leinco, Beiing, China). Briefly, 1×10^5 cells were resuspended in binding buffer and stained with 5 µL Annexin V-FITC and 10 µL propidium iodide (PI) for 15 min in the dark. The stained cells were analyzed using flow cytometry (CytoFLEX, Beckman, High Wycombe, UK).

Iron Assay

The intracellular Fe^{2+} concentration was determined using an Iron Assay kit (MAK025, Merck, Darmstadt, Germany). Approximately 5×10^4 cells were homogenized in Iron Assay Buffer and centrifuged at 16,000 g for 10 min. The supernatant was mixed with the Assay Buffer, Iron Reducer, and Iron Probe in a 96-well plate and incubated at 37 °C for 60 min in the dark. Absorbance was measured at 593 nm using a microplate reader to quantify Fe^{2+} levels.

Measurement of Lipid Peroxidation

Lipid peroxidation was assessed using C11-BODIPY 581/591 dye (NBS5113, Nonin Biological Technology Co., Ltd., Shanghai, China). A 10 µM working solution was prepared in preheated serum-free medium. Treated cells (1×10^5) were incubated with 1 mL of the working solution for

Table 1. Antibodies used in this study.

Name	Catalog No.	Molecular Weight (kDa)	Clone ID	Dilution	Manufacturer (UK)
GPX4	ab125066	17	EPNCIR144	1:1000	Abcam
ACSL4	ab155282	62	EPR8640	1:1000	Abcam
p-eIF2α	ab32157	34/36	E90	1:1000	Abcam
eIF2α	ab169528	65	EPR11042	1:1000	Abcam
β-actin	ab8226	42	mAbcam 8226	1:10,000	Abcam
Goat anti-rabbit	ab205718	—	—	1:2000	Abcam
Goat anti-mouse	ab205719	—	—	1:2000	Abcam

Abbreviation: GPX4, glutathione peroxidase 4; ACSL4, acyl-CoA synthetase long-chain family member 4; eIF2α, eukaryotic translation initiation factor 2α.

15 min, centrifuged at 400 g, and resuspended in phosphate-buffered saline (PBS, AC13319, Acmec, Shanghai, China). Fluorescence was analyzed using flow cytometry to determine lipid ROS accumulation.

Western Blotting

Tumor tissues and RCC cells were lysed using radioimmunoprecipitation assay (RIPA) buffer (AC13971, Acmec, Shanghai, China), and the resulting lysates were analyzed for protein concentration using a bicinchoninic acid (BCA) assay kit (GK10009, GLPBIO, Shanghai, China). Equal amounts of protein were separated by sodium dodecyl sulfate-polyacrylamide gel electrophoresis (SDS-PAGE) (AC13342, Acmec, Shanghai, China) and subsequently transferred to polyvinylidene fluoride (PVDF) membranes. The membranes were blocked with 5% bovine serum albumin (BSA) blocking buffer (GF15660, GLPBIO, Shanghai, China) for 1 h. Membranes were then incubated with primary antibodies against the target proteins (Table 1) at 4 °C for 24 h, followed by incubation with secondary antibodies at room temperature for 2 h. Detection was performed using enhanced chemiluminescence (ECL) reagents (AC138942, Acmec, Shanghai, China) and imaged using a JP-K300 imaging system (Jiapeng, Guangzhou, China). β-actin was used as the internal control. Band intensities were quantified with ImageJ software (Version 1.53, National Institutes of Health, Bethesda, MD, USA) and normalized to β-actin (loading control). Data are expressed as fold change relative to the control group.

Animals

Ninety male BALB/c nude mice (20–23 g, 6–8 weeks old; Hangzhou Medical College) were housed under controlled conditions with a 12-h light/dark cycle and 50% humidity. All experimental procedures were approved by the Ethics Committee of Shaoxing People's Hospital for Experimental Animal Welfare (Approval No. 2023Z008). The orthotopic RCC tumor model was established in BALB/c nude mice as previously described [20]. Briefly, under inhalational anesthesia with 1–3% isoflurane (R510-22-10, RWD, Shenzhen, China), the left kidney was exposed, and 45 mice each received an injection of either 769-P or 786-O cells (5×10^6) under the renal capsule.

After tumor implantation, the 45 mice were randomly assigned to three groups: Control, Sorafenib, and Sorafenib + Isrib. Three days after model establishment, the mice received intraperitoneal injections of PBS, Sorafenib (20 mg/kg) [21], or Isrib (2.5 mg/kg) [22]. Each experimental group (Control, Sorafenib, Sorafenib + Isrib) consisted of 15 mice and was subdivided into two subsets. One subset (n = 5 per group) was anesthetized with 1–3% isoflurane (R510-22-10, RWD, Shenzhen, China) on day 15 after treatment initiation, and tumor tissues were collected after euthanasia by cervical dislocation. The remaining mice (n = 10 per group) were used for survival analysis and were monitored until day 35.

Histological Analysis

Tumor tissues were fixed, paraffin-embedded, and sectioned into 5 µm slices. Sections were deparaffinized in xylene, rehydrated through a graded series of ethanol (100%, 90%, 80%, and 70%), and rinsed with distilled water. After PBS washing, sections were permeabilized with Triton X-100 (T17048, Saint-Bio, Shanghai, China) for 10 min, rinsed again with PBS, and incubated with endogenous peroxidase blocking buffer (P0100A, Beyotime, Shanghai, China) for 10 min at room temperature. Antigen retrieval was performed using citrate buffer (M20215, Saint-Bio, Shanghai, China).

The sections were then incubated with 4-hydroxynonenal (4-HNE) antibody (ab48506, Abcam, Cambridge, UK) at 4 °C for 24 h, followed by incubation with goat anti-mouse IgG H&L (HRP) secondary antibody (ab205719, Abcam, Cambridge, UK) at room temperature. Positive immunostaining was visualized as brown signals using a 3,3'-Diaminobenzidine (DAB) chromogenic kit (R23495, Saint-Bio, Shanghai, China). Sections were examined under an optical microscope (400×, N300M, Yongxin, Beijing, China). The percentage of 4-HNE-positive cells was determined as follows:

4-HNE-positive rate (%) = (Number of positive cells / Number of total cells) × 100

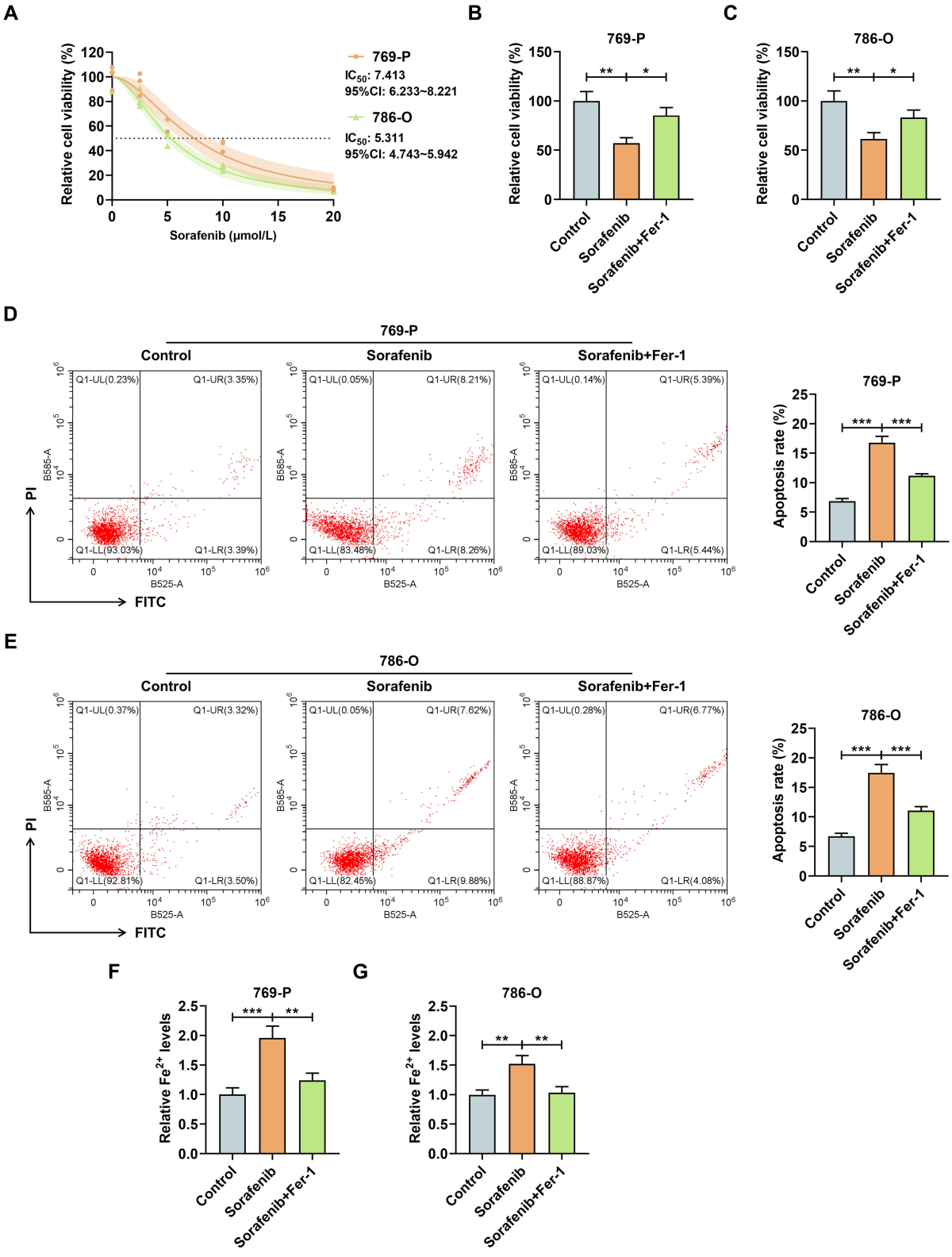

Fig. 1. Effects of Fer-1 and sorafenib on RCC cell viability, apoptosis, and intracellular Fe^{2+} levels. RCC cells (769-P and 786-O) were divided into three groups: Control group (normal culture), Sorafenib group (treatment with 10 μM sorafenib) and Sorafenib + Fer-1 group (treatment with 10 μM sorafenib and 5 μM ferroptosis inhibitor Fer-1). (A–C) Cell viability assessed by the CCK-8 assay. (D,E) Apoptosis analyzed by flow cytometry. (F,G) Intracellular Fe^{2+} levels measured using a commercial kit. Data are presented as mean ± standard deviation from at least three independent experiments (n = 3). $*p < 0.05$, $**p < 0.01$, $***p < 0.001$. Abbreviations: RCC, renal cell cancer; CCK-8, Cell Counting Kit 8; Fer-1, ferrostatin-1.

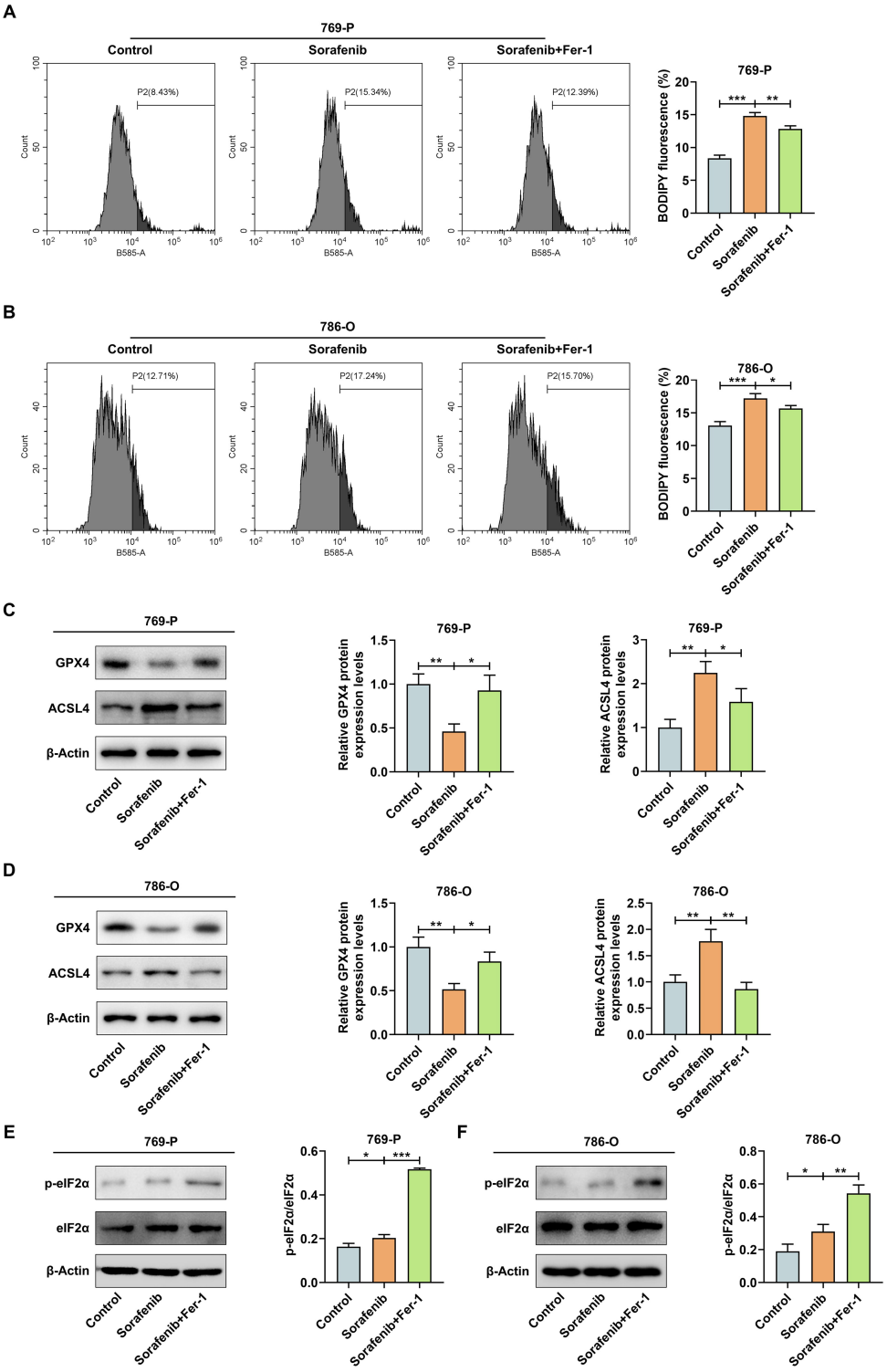

Fig. 2. Effects of Fer-1 and sorafenib on lipid peroxidation, ferroptosis-related protein expression, and the p-eIF2α/eIF2α pathway. RCC cells (769-P and 786-O) were divided into three groups: Control group (normal culture), Sorafenib group (treatment with 10 μM sorafenib), and Sorafenib + Fer-1 group (treatment with 10 μM sorafenib and 5 μM ferroptosis inhibitor Fer-1). (A,B) Lipid peroxidation in RCC cells detected using C11-BODIPY. (C,D) Expression of ferroptosis-related proteins GPX4 and ACSL4 analyzed by Western blotting (β-actin as the internal control). (E,F) Expression of eIF2α and p-eIF2α analyzed by Western blotting (β-actin as the internal control). Data are presented as mean ± standard deviation from at least three independent experiments (n = 3). *$p < 0.05$, **$p < 0.01$, ***$p < 0.001$. Abbreviations: RCC, renal cell cancer; Fer-1, ferrostatin-1; GPX4, glutathione peroxidase 4; ACSL4, acyl-CoA synthetase long-chain family member 4; eIF2α, eukaryotic translation initiation factor 2α.

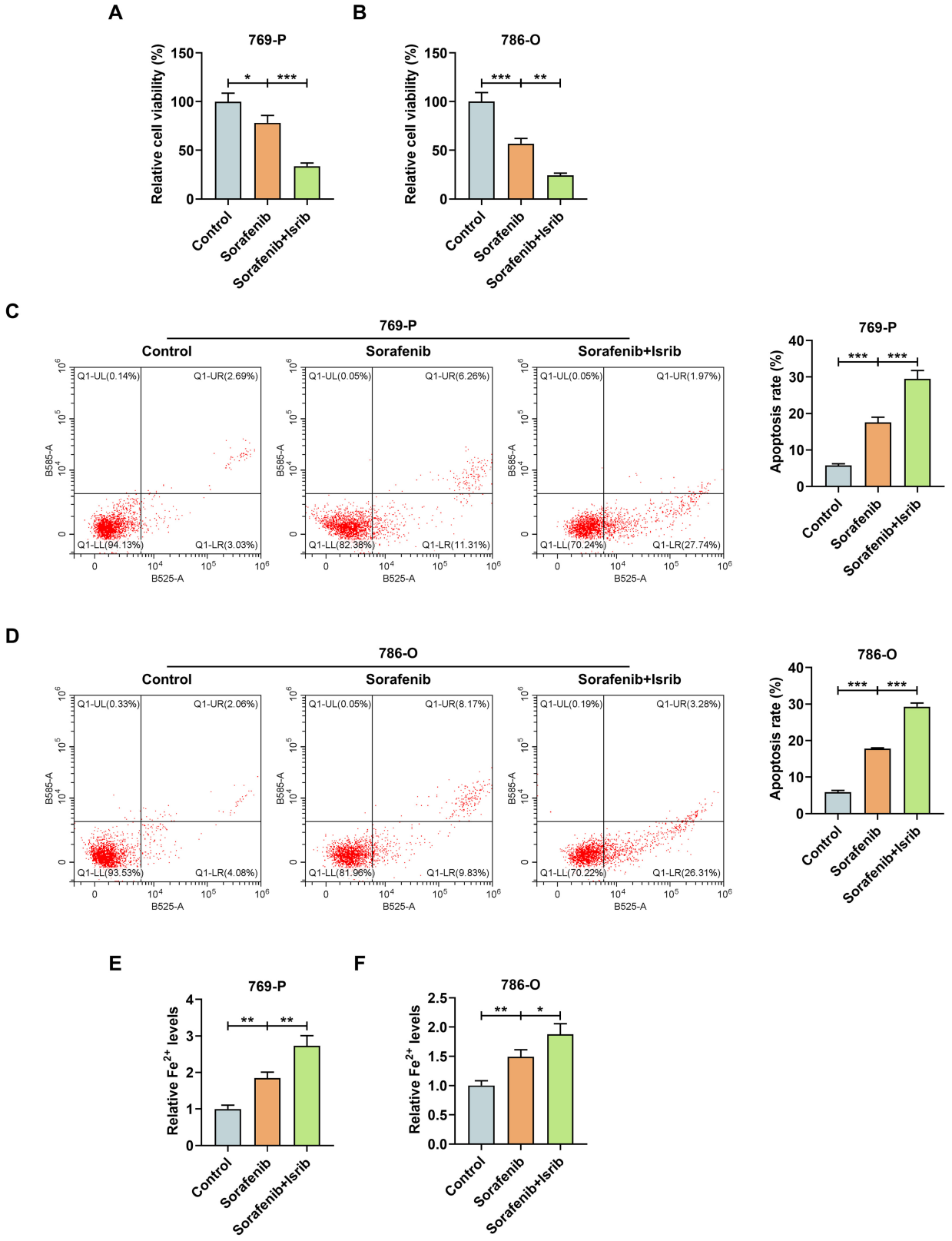

Fig. 3. Effects of Isrib on the viability, apoptosis, and Fe^{2+} levels of RCC cells. RCC cells (769-P and 786-O) were divided into three groups: Control group (normal culture), Sorafenib group (treatment with 10 μM sorafenib), and Sorafenib + Isrib group (treatment with 10 μM sorafenib and 200 nM eIF2α phosphorylation inhibitor Isrib). (A,B) Cell viability assessed by the CCK-8 assay. (C,D) Apoptosis analyzed by flow cytometry. (E,F) Intracellular Fe^{2+} levels measured using a commercial kit. Data are presented as mean ± standard deviation from at least three independent experiments (n = 3). *$p < 0.05$, **$p < 0.01$, ***$p < 0.001$. Abbreviations: RCC, renal cell cancer; CCK-8, Cell Counting Kit 8; eIF2α, eukaryotic translation initiation factor 2α.

Statistical Analyses

GraphPad Prism v8.0 (GraphPad Software, San Diego, CA, USA) was employed for all statistical analyses. Quantitative data are presented as the mean ± standard deviation (SD) from at least three independent experiments. Each data point represents a single measurement from one independent experiment. Comparisons between two groups were performed using an independent-sample *t*-test, while comparisons among multiple groups were analyzed by one-way analysis of variance (ANOVA), followed by Tukey's post hoc test. Two-factor ANOVA with Tukey's multiple comparisons was used to analyze the influence of two independent factors. Kaplan-Meier survival curves were analyzed using the log-rank test. Statistical significance was set at $p < 0.05$.

Results

Sorafenib Induces Ferroptosis in RCC Cells

During the screening for the optimal concentration of sorafenib to inhibit cell viability, we found that sorafenib exhibited a dose-dependent inhibitory effect on the viability of 769-P and 786-O cells (Fig. 1A). As the concentration increased, cell viability gradually decreased (Fig. 1A). Based on these results, we selected 10 μM, the concentration closest to the IC50 value, for the subsequent experiments. Next, RCC cells were treated with sorafenib and the ferroptosis inhibitor Fer-1. Sorafenib significantly inhibited cell viability (Fig. 1B,C, $p < 0.01$) and promoted apoptosis (Fig. 1D,E, $p < 0.001$). Moreover, sorafenib treatment led to an increase in Fe^{2+} content (Fig. 1F,G, $p < 0.01$) and lipid peroxidation (Fig. 2A,B, $p < 0.001$) in RCC cells, accompanied by downregulation of glutathione peroxidase 4 (GPX4) protein and upregulation of acyl-CoA synthetase long-chain family member 4 (ACSL4) protein expression (Fig. 2C,D, $p < 0.01$). Notably, all these effects of sorafenib were reversed by Fer-1 treatment (Fig. 1B–G and Fig. 2A–D, $p < 0.05$). Furthermore, sorafenib-induced an increase in the p-eIF2α/eIF2α ratio in RCC cells, and this effect was further enhanced by Fer-1 (Fig. 2E,F, $p < 0.05$).

EIF2α Phosphorylation Inhibitor Isrib Enhances the Pro-Ferroptotic Effect of Sorafenib in RCC Cells

To further examine the role of eIF2α phosphorylation in sorafenib-induced ferroptosis, we used the eIF2α phosphorylation inhibitor Isrib. We found that the effects of sorafenib on RCC cells, including inhibition of cell viability (Fig. 3A,B, $p < 0.05$), promotion of apoptosis (Fig. 3C,D, $p < 0.001$), elevation of Fe^{2+} content (Fig. 3E,F, $p < 0.01$), and enhancement of lipid peroxidation (Fig. 4A,B, $p < 0.05$), were all augmented by Isrib co-treatment. Similarly, sorafenib-induced downregulation of GPX4 protein and upregulation of ACSLC4 protein (Fig. 4C,D, $p < 0.05$) were further enhanced by Isrib. Western blot analysis revealed that sorafenib promoted the upregulation of the p-eIF2α/eIF2α ratio, while Isrib suppressed this regulatory effect (Fig. 4E,F, $p < 0.01$).

Isrib Enhances the Anti-Tumor and Pro-Ferroptotic Effects of Sorafenib In Vivo

To further investigate whether Isrib enhances the anticancer efficacy of sorafenib *in vivo*, animal experiments were conducted. Sorafenib treatment significantly inhibited tumor growth and prolonged mouse survival (Fig. 5A–E, $p < 0.05$). Compared with sorafenib alone, the combination of sorafenib and Isrib resulted in smaller tumor volume ($p < 0.05$) and extended survival time (Fig. 5A–E). Moreover, Isrib further amplified sorafenib-induced lipid peroxidation, downregulated GPX4 protein, and upregulated ACSL4 protein (Fig. 6A–C, $p < 0.05$). The increase in p-eIF2α/eIF2α ratio induced by sorafenib was also reversed by Isrib (Fig. 6D,E, $p < 0.01$).

Discussion

Currently, it is recognized that the mechanisms underlying sorafenib resistance include five key aspects: non-coding RNA-mediated resistance, upregulation of pro-angiogenic signaling pathways, activation of the rapidly accelerated fibrosarcoma (RAF)/mitogen-activated protein (MEK)/extracellular signal-regulated kinase (ERK) and phosphoinositide 3-kinase (PI3K)/protein kinase B (AKT)/mammalian target of rapamycin (mTOR) pathways, pharmacokinetic drug metabolism, and the hypoxic tumor microenvironment [5]. This study extends beyond these five aspects and explores how to enhance the sensitivity of RCC cells to sorafenib from the perspective of eIF2α phosphorylation.

We first evaluated ferroptosis in RCC cells following sorafenib treatment. Ferroptosis is a recently identified, iron-dependent form of programmed cell death characterized by the generation of ROS through the Fenton reaction, which promotes lipid peroxidation. In this study, sorafenib not only increased the levels of Fe^{2+} and the accumulation of lipid peroxide, but also regulated the expression of GPX4 and ACSL4. The principal function of GPX4 is to limit lipid peroxidation, thereby preventing ferroptosis [23]. ACSL4, a member of the ACSL family, catalyzes the metabolic processing of long-chain fatty acids and serves as an essential regulator of lipid metabolism during ferroptosis [24]. Previous research has shown that ACSL4-mediated regulation of ferroptosis contributes to sorafenib resistance in hepatocellular carcinoma [25]. Similarly, inhibition of GPX4 sensitizes hepatocellular carcinoma cells to sorafenib-induced ferroptosis [26]. In the present study, we employed the ferroptosis inhibitor Fer-1, which has been shown to upregulate GPX4 and downregulate ACSL4 in RCC cells [27]. Interestingly, Fer-1 reversed the effects of sorafenib on Fe^{2+} levels, lipid peroxide accumulation, and ferroptosis-related proteins (GPX4 and ACSL4) in RCC cells, indicating that

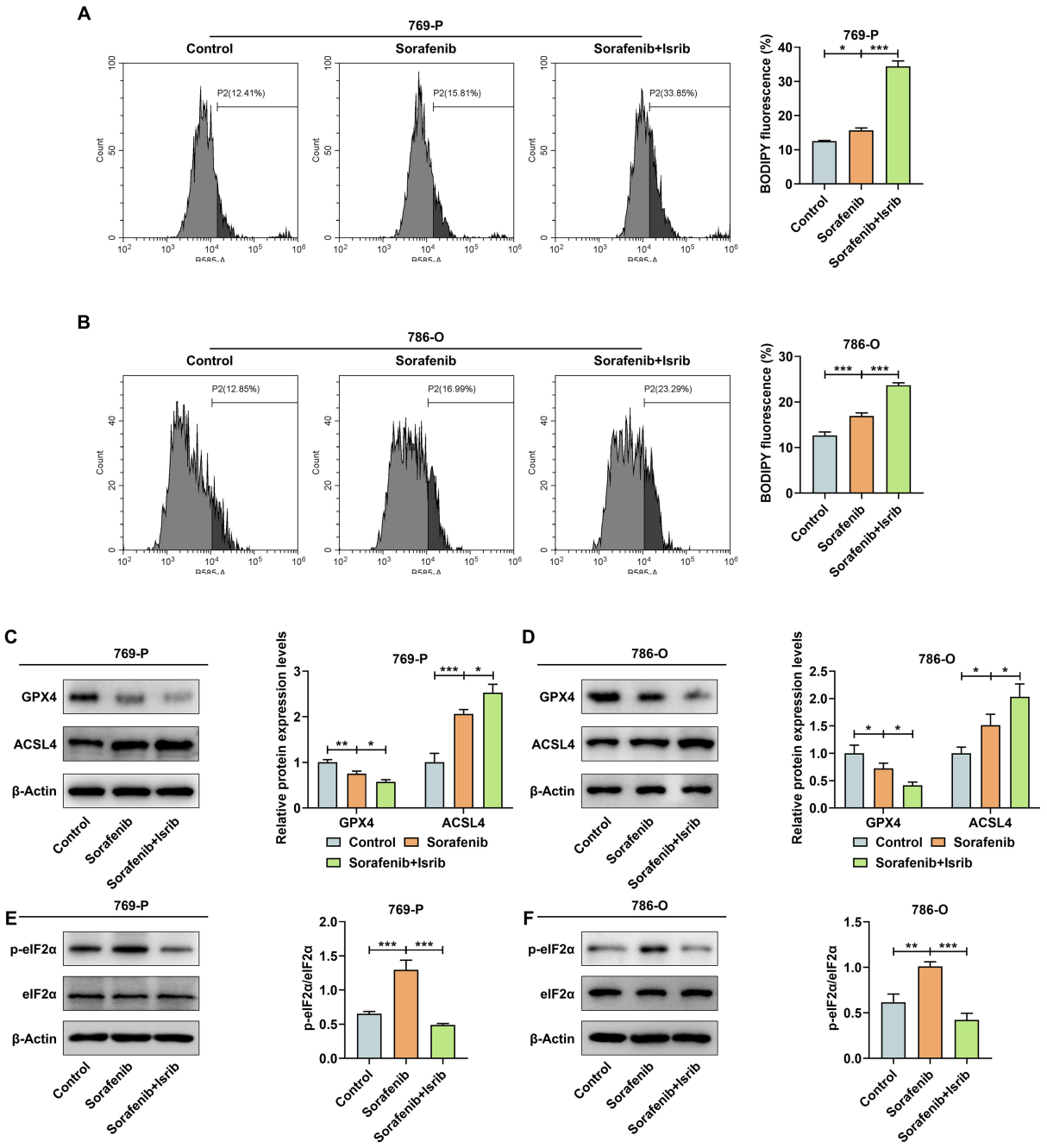

Fig. 4. Effects of Isrib on lipid peroxidation, ferroptosis-related protein expression, and the p-eIF2α/eIF2α pathway in RCC cells. RCC cells (769-P and 786-O) were divided into three groups: Control group (normal culture), Sorafenib group (treatment with 10 µM Sorafenib), and Sorafenib + Isrib group (treatment with 10 µM Sorafenib and 200 nM EIF2α phosphorylation inhibitor Isrib). (A,B) Lipid peroxidation levels in RCC cells measured using C11-BODIPY fluorescence. (C,D) Expression of ferroptosis-related proteins GPX4 and ACSL4 (Western blotting, β-actin as internal control). (E,F) The expressions of eIF2α and p-eIF2α (Western blotting, β-actin as the internal control). Data are presented as mean ± standard deviation from at least three independent experiments (n = 3). *$p < 0.05$, **$p < 0.01$, ***$p < 0.001$. Abbreviations: RCC, renal cell cancer; GPX4, glutathione peroxidase 4; ACSL4, acyl-CoA synthetase long-chain family member 4; eIF2α, eukaryotic translation initiation factor 2α.

inhibition of ferroptosis can indeed influence the therapeutic efficacy of sorafenib in RCC cells.

Next, we focused on the causal relationship between eIF2α phosphorylation and the response to sorafenib. We found that sorafenib promoted eIF2α phosphorylation, which may represent a stress response of RCC cells to chemotherapy drugs, as the eIF2α phosphorylation participates in the assembly of stress granules (SGs) [28]. Formation of SGs has been reported to reduce cellular sensitivity to sorafenib [29]. Therefore, sorafenib-induced

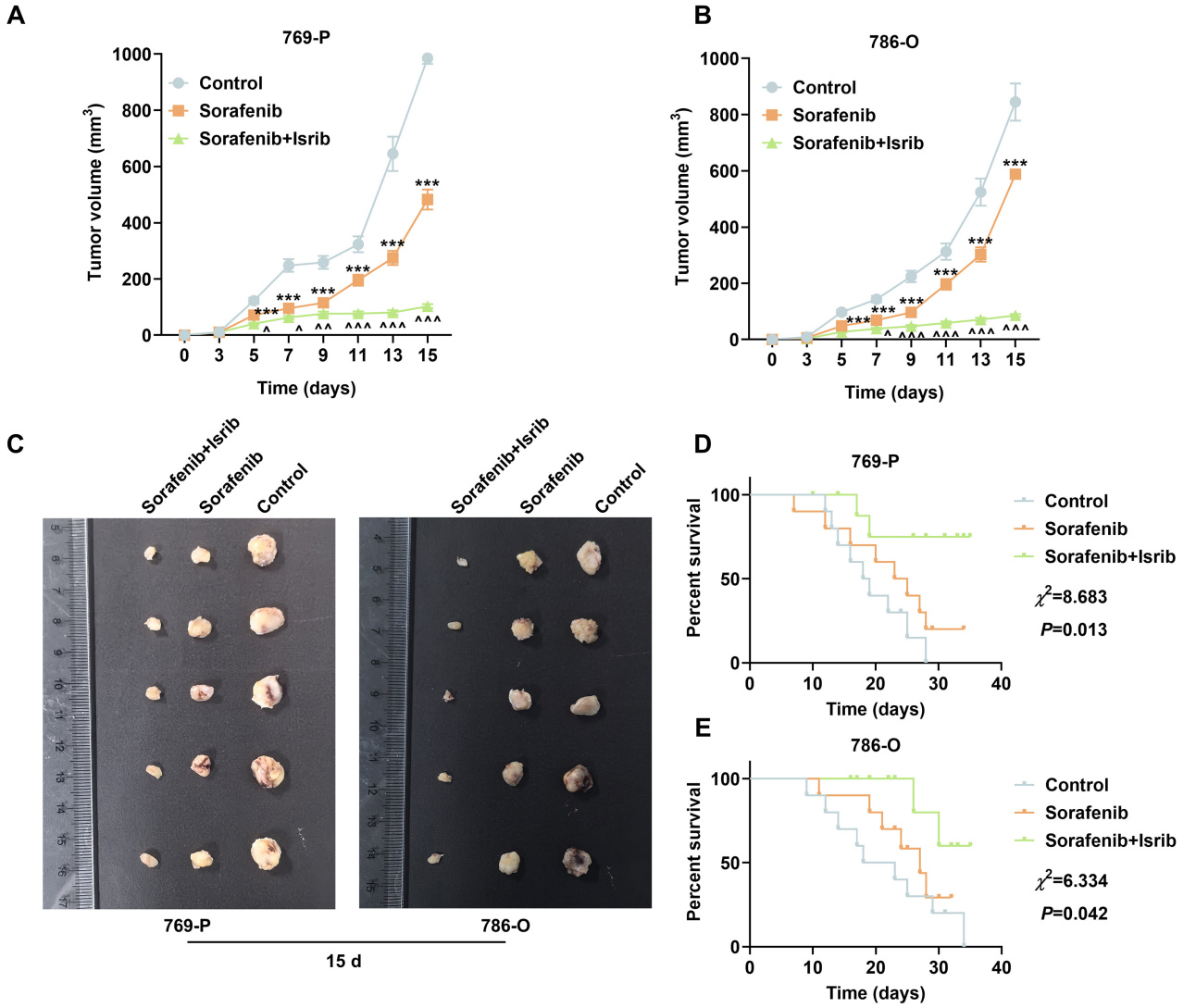

Fig. 5. Effects of Isrib on xenograft tumor growth and survival in tumor-bearing mice. An orthotopic renal cell carcinoma was established in BALB/c nude mice. Three days later, the mice received intraperitoneal injections of PBS, sorafenib (20 mg/kg) or Isrib (2.5 mg/kg). (A,B) Tumor volume in different treatment groups. (C) Representative images of xenograft tumors under various treatments. (D,E) Kaplan-Meier survival curves of tumor-bearing mice monitored daily until death. Data are presented as mean ± standard deviation from at least three independent experiments (n = 5 for (A–C); n = 10 for (D,E)). ***$p < 0.001$ vs. Control group; $^{\wedge}p < 0.05$, $^{\wedge\wedge}p < 0.01$, $^{\wedge\wedge\wedge}p < 0.001$ vs. Sorafenib group. Abbreviations: PBS, phosphate-buffered saline.

eIF2α phosphorylation may eventually suppress the sensitivity of RCC cells to sorafenib. eIF2α phosphorylation also contributes to tumor progression in various malignancies; for instance, it promotes the growth of pancreatic ductal adenocarcinoma [30] and mediates resistance to gefitinib in ovarian cancer cells [31]. Notably, inhibition of eIF2α phosphorylation has been shown to induce apoptosis in RCC cells [32], possibly because eIF2α facilitates tumor cells' adaptation to hypoxia through the ATF4/C/EBP-homologous protein (CHOP) signaling pathway, thus promoting the survival of tumor cells [33]. Consistent with these findings, our results demonstrate that Isrib further enhances sorafenib-induced apoptosis in RCC cells. Previous research also reported that eIF2α mediates ferroptosis via the eIF2α-ATF4 pathway [34], and modulation of this pathway can enhance ferroptosis in triple-negative breast cancer cells. The well-established eIF2α-ATF4 axis thus represents a compelling mechanism through which eIF2α phosphorylation indirectly regulates ferroptosis mediators such as GPX4 and ACSL4, potentially by controlling the cellular redox balance and lipid metabolism profile.

Isrib has been reported to synergize with doxorubicin to suppress tumor growth in triple-negative breast cancer [35]. Moreover, Isrib can sensitize tumor cells to photothermal therapy by inhibiting SG formation [36]. Consistent with these findings, we observed that Isrib enhanced the effects of sorafenib on Fe^{2+} levels, lipid peroxide accumulation, and ferroptosis-related proteins, indicating that inhi-

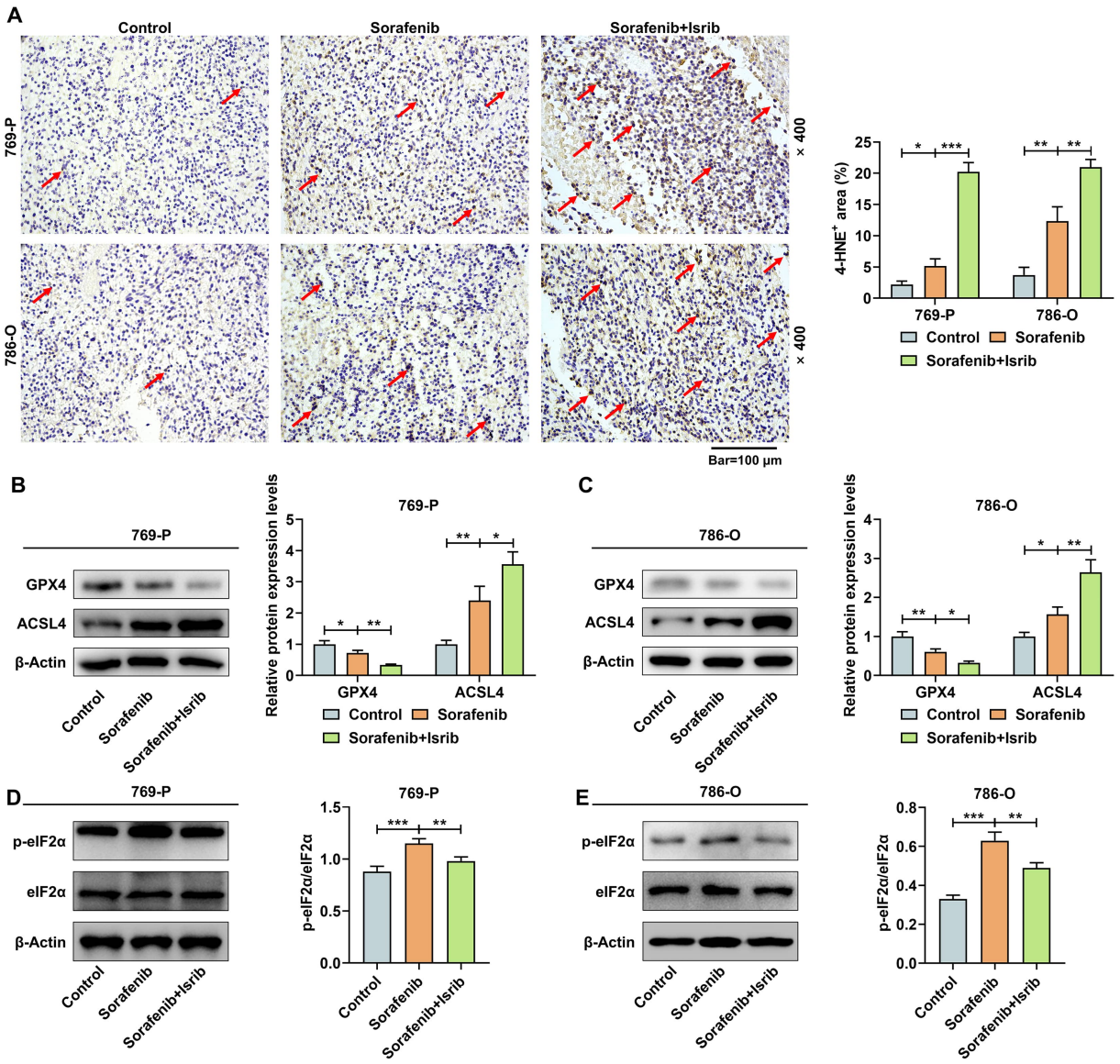

Fig. 6. Effects of Isrib on lipid peroxidation, ferroptosis-related proteins, and p-eIF2α/eIF2α expression in tumor-bearing mice. (A) 4-HNE staining showing lipid peroxidation in tumor tissues (Scale: 100 μm, × 400). Red arrows indicate representative 4-HNE-positive cells (brown granule). (B,C) Expression of ferroptosis-related proteins GPX4 and ACSL4 (Western blotting, β-actin as the internal control). (D,E) Expression levels of eIF2α and p-eIF2α (Western blotting, β-actin as the internal control). Data are presented as mean ± standard deviation from at least three independent experiments (n = 3). *$p < 0.05$, **$p < 0.01$, ***$p < 0.001$. Abbreviations: eIF2α, eukaryotic translation initiation factor 2α; 4-HNE, 4-hydroxynonenal; GPX4, glutathione peroxidase 4; ACSL4, acyl-CoA synthetase long-chain family member 4.

bition of phosphorylated eIF2α can facilitate the induction of ferroptosis in RCC by sorafenib. Finally, we verified the synergistic effect of Isrib on the therapeutic efficacy of sorafenib in animal experiments.

However, this study has several limitations. It was primarily conducted using cell lines and nude mouse models, and therefore lacks validation in clinical samples. Additionally, the specific molecular interactions between eIF2α phosphorylation and ferroptosis-related proteins (e.g., GPX4, ACSL4) warrant further exploration to elucidate the underlying mechanisms in greater detail. Additionally, the detection of ferroptosis markers in this study was limited to key proteins (e.g., GPX4, ACSL4). Future research should incorporate more direct metabolic indicators, such as lipid ROS quantification, to provide a more comprehensive understanding of ferroptosis regulation in RCC.

Conclusion

In summary, our findings demonstrate that the inhibition of eIF2α phosphorylation promotes the induction

of ferroptosis in RCC cells by sorafenib, offering a novel therapeutic direction for overcoming sorafenib resistance in RCC. Moreover, while the concentrations used in this study effectively supported our central hypothesis, future dose-response investigations are warranted to delineate the precise synergistic window and minimize potential cytotoxicity, thereby enhancing the therapeutic index of this combinatorial approach.

Availability of Data and Materials

The analyzed data sets generated during the study are available from the corresponding author on reasonable request.

Author Contributions

LY and CZ designed the research study. JY and YR performed the research. KG and CS collected and analyzed the data. YR has been involved in drafting the manuscript and all authors have been involved in revising it critically for important intellectual content. All authors gave final approval of the version to be published. All authors have participated sufficiently in the work to take public responsibility for appropriate portions of the content and agreed to be accountable for all aspects of the work.

Ethics Approval and Consent to Participate

The Ethics Committee of Shaoxing People's Hospital for Experimental Animals Welfare (2023Z008) authorized all procedures involving animals.

Acknowledgment

Not applicable.

Funding

This work was supported by the Zhejiang Provincial Medical and Health Science and Technology Program under Grant [number 2023KY354].

Conflict of Interest

The authors declare no conflict of interest.

References

[1] Sung H, Ferlay J, Siegel RL, Laversanne M, Soerjomataram I, Jemal A, *et al*. Global Cancer Statistics 2020: GLOBOCAN Estimates of Incidence and Mortality Worldwide for 36 Cancers in 185 Countries. CA: A Cancer Journal for Clinicians. 2021; 71: 209–249. https://doi.org/10.3322/caac.21660.

[2] Bahadoram S, Davoodi M, Hassanzadeh S, Bahadoram M, Barahman M, Mafakher L. Renal cell carcinoma: an overview of the epidemiology, diagnosis, and treatment. Giornale Italiano Di Nefrologia. 2022; 39: 2022–vol3.

[3] Pontes O, Oliveira-Pinto S, Baltazar F, Costa M. Renal cell carcinoma therapy: Current and new drug candidates. Drug Discovery Today. 2022; 27: 304–314. https://doi.org/10.1016/j.drudis.2021.07.009.

[4] Escudier B, Worden F, Kudo M. Sorafenib: key lessons from over 10 years of experience. Expert Review of Anticancer Therapy. 2019; 19: 177–189. https://doi.org/10.1080/14737140.2019.1559058.

[5] He Y, Luo Y, Huang L, Zhang D, Wang X, Ji J, *et al*. New frontiers against sorafenib resistance in renal cell carcinoma: From molecular mechanisms to predictive biomarkers. Pharmacological Research. 2021; 170: 105732. https://doi.org/10.1016/j.phrs.2021.105732.

[6] Liu Y, Liu X, Luo M, Li Y, Li H. HBx Modulates Drug Resistance of Sorafenib-Resistant Hepatocellular Carcinoma Cells. Discovery Medicine. 2023; 35: 1035–1042. https://doi.org/10.24976/Discov.Med.202335179.99.

[7] Guo L, Hu C, Yao M, Han G. Mechanism of sorafenib resistance associated with ferroptosis in HCC. Frontiers in Pharmacology. 2023; 14: 1207496. https://doi.org/10.3389/fphar.2023.1207496.

[8] Tang D, Chen X, Kang R, Kroemer G. Ferroptosis: molecular mechanisms and health implications. Cell Research. 2021; 31: 107–125. https://doi.org/10.1038/s41422-020-00441-1.

[9] Yang L, Fan Y, Zhang Q. Targeting ferroptosis in renal cell carcinoma: Potential mechanisms and novel therapeutics. Heliyon. 2023; 9: e18504. https://doi.org/10.1016/j.heliyon.2023.e18504.

[10] Lai Y, Zeng T, Liang X, Wu W, Zhong F, Wu W. Cell death-related molecules and biomarkers for renal cell carcinoma targeted therapy. Cancer Cell International. 2019; 19: 221. https://doi.org/10.1186/s12935-019-0939-2.

[11] Shiota M, Eto M, Yokomizo A, Tada Y, Takeuchi A, Masubuchi D, *et al*. Sorafenib with doxorubicin augments cytotoxicity to renal cell cancer through PERK inhibition. International Journal of Oncology. 2010; 36: 1521–1531. https://doi.org/10.3892/ijo_00000639.

[12] Boye E, Grallert B. eIF2α phosphorylation and the regulation of translation. Current Genetics. 2020; 66: 293–297. https://doi.org/10.1007/s00294-019-01026-1.

[13] Le HT, Yu J, Ahn HS, Kim MJ, Chae IG, Cho HN, *et al*. eIF2α phosphorylation-ATF4 axis-mediated transcriptional reprogramming mitigates mitochondrial impairment during ER stress. Molecules and Cells. 2025; 48: 100176. https://doi.org/10.1016/j.mocell.2024.100176.

[14] Zhou B, Lu D, Wang A, Cui J, Zhang L, Li J, *et al*. Endoplasmic reticulum stress promotes sorafenib resistance via miR-188-5p/hnRNPA2B1-mediated upregulation of PKM2 in hepatocellular carcinoma. Molecular Therapy. Nucleic Acids. 2021; 26: 1051–1065. https://doi.org/10.1016/j.omtn.2021.09.014.

[15] Wang SF, Chen MS, Chou YC, Ueng YF, Yin PH, Yeh TS, *et al*. Mitochondrial dysfunction enhances cisplatin resistance in human gastric cancer cells via the ROS-activated GCN2-eIF2α-ATF4-xCT pathway. Oncotarget. 2016; 7: 74132–74151. https://doi.org/10.18632/oncotarget.12356.

[16] Koppula P, Zhuang L, Gan B. Cystine transporter SLC7A11/xCT in cancer: ferroptosis, nutrient dependency, and cancer therapy. Protein & Cell. 2021; 12: 599–620. https://doi.org/10.1007/s13238-020-00789-5.

[17] Wang SF, Wung CH, Chen MS, Chen CF, Yin PH, Yeh TS, *et al*. Activated Integrated Stress Response Induced by Salubrinal Promotes Cisplatin Resistance in Human Gastric Cancer Cells via Enhanced xCT Expression and Glutathione Biosynthesis. International Journal of Molecular Sciences. 2018; 19: 3389. https://doi.org/10.3390/ijms19113389.

[18] Li Y, Yan J, Zhao Q, Zhang Y, Zhang Y. ATF3 promotes ferroptosis in sorafenib-induced cardiotoxicity by suppressing Slc7a11

expression. Frontiers in Pharmacology. 2022; 13: 904314. https://doi.org/10.3389/fphar.2022.904314.

[19] Ohto T, Konishi M, Tanaka H, Onomoto K, Yoneyama M, Nakai Y, *et al*. Inhibition of the Inflammatory Pathway Enhances Both the in Vitro and in Vivo Transfection Activity of Exogenous in Vitro-Transcribed mRNAs Delivered by Lipid Nanoparticles. Biological & Pharmaceutical Bulletin. 2019; 42: 299–302. https://doi.org/10.1248/bpb.b18-00783.

[20] de Souza Braga M, Chaves KB, Chammas R, Schor N, Bellini MH. Endostatin neoadjuvant gene therapy extends survival in an orthotopic metastatic mouse model of renal cell carcinoma. Biomedicine & Pharmacotherapy. 2012; 66: 237–241. https://doi.org/10.1016/j.biopha.2011.11.002.

[21] Li ZJ, Dai HQ, Huang XW, Feng J, Deng JH, Wang ZX, *et al*. Artesunate synergizes with sorafenib to induce ferroptosis in hepatocellular carcinoma. Acta Pharmacologica Sinica. 2021; 42: 301–310. https://doi.org/10.1038/s41401-020-0478-3.

[22] Chen G, Yang X, He Y, Tang Y, Tian R, Huang W, *et al*. Inhibiting alpha subunit of eukaryotic initiation factor 2 dephosphorylation protects injured hepatocytes and reduces hepatocyte proliferation in acute liver injury. Croatian Medical Journal. 2019; 60: 532–544. https://doi.org/10.3325/cmj.2019.60.532.

[23] Liu J, Kang R, Tang D. Signaling pathways and defense mechanisms of ferroptosis. The FEBS Journal. 2022; 289: 7038–7050. https://doi.org/10.1111/febs.16059.

[24] Yang Y, Zhu T, Wang X, Xiong F, Hu Z, Qiao X, *et al*. ACSL3 and ACSL4, Distinct Roles in Ferroptosis and Cancers. Cancers. 2022; 14: 5896. https://doi.org/10.3390/cancers14235896.

[25] Lu Y, Chan YT, Tan HY, Zhang C, Guo W, Xu Y, *et al*. Epigenetic regulation of ferroptosis via ETS1/miR-23a-3p/ACSL4 axis mediates sorafenib resistance in human hepatocellular carcinoma. Journal of Experimental & Clinical Cancer Research. 2022; 41: 3. https://doi.org/10.1186/s13046-021-02208-x.

[26] Wang Q, Bin C, Xue Q, Gao Q, Huang A, Wang K, *et al*. GSTZ1 sensitizes hepatocellular carcinoma cells to sorafenib-induced ferroptosis via inhibition of NRF2/GPX4 axis. Cell Death & Disease. 2021; 12: 426. https://doi.org/10.1038/s41419-021-03718-4.

[27] Du Y, Zhao HC, Zhu HC, Jin Y, Wang L. Ferroptosis is involved in the anti-tumor effect of lycorine in renal cell carcinoma cells. Oncology Letters. 2021; 22: 781. https://doi.org/10.3892/ol.2021.13042.

[28] Wang F, Li J, Fan S, Jin Z, Huang C. Targeting stress granules: A novel therapeutic strategy for human diseases. Pharmacological Research. 2020; 161: 105143. https://doi.org/10.1016/j.phrs.2020.105143.

[29] Adjibade P, St-Sauveur VG, Quevillon Huberdeau M, Fournier MJ, Savard A, Coudert L, *et al*. Sorafenib, a multikinase inhibitor, induces formation of stress granules in hepatocarcinoma cells. Oncotarget. 2015; 6: 43927–43943. https://doi.org/10.18632/oncotarget.5980.

[30] Li Z, Ge Y, Dong J, Wang H, Zhao T, Wang X, *et al*. BZW1 Facilitates Glycolysis and Promotes Tumor Growth in Pancreatic Ductal Adenocarcinoma Through Potentiating eIF2α Phosphorylation. Gastroenterology. 2022; 162: 1256–1271.e14. https://doi.org/10.1053/j.gastro.2021.12.249.

[31] Kim TW, Lee HG. 6-Shogaol Overcomes Gefitinib Resistance via ER Stress in Ovarian Cancer Cells. International Journal of Molecular Sciences. 2023; 24: 2639. https://doi.org/10.3390/ijms24032639.

[32] Han KS, Li N, Raven PA, Fazli L, Frees S, Ettinger S, *et al*. Inhibition of endoplasmic reticulum chaperone protein glucose-regulated protein 78 potentiates anti-angiogenic therapy in renal cell carcinoma through inactivation of the PERK/eIF2α pathway. Oncotarget. 2015; 6: 34818–34830. https://doi.org/10.18632/oncotarget.5397.

[33] Rozpedek W, Pytel D, Mucha B, Leszczynska H, Diehl JA, Majsterek I. The Role of the PERK/eIF2α/ATF4/CHOP Signaling Pathway in Tumor Progression During Endoplasmic Reticulum Stress. Current Molecular Medicine. 2016; 16: 533–544. https://doi.org/10.2174/1566524016666160523143937.

[34] Lee YS, Lee DH, Choudry HA, Bartlett DL, Lee YJ. Ferroptosis-Induced Endoplasmic Reticulum Stress: Cross-talk between Ferroptosis and Apoptosis. Molecular Cancer Research. 2018; 16: 1073–1076. https://doi.org/10.1158/1541-7786.MCR-18-0055.

[35] Wang X, Chen T, Li C, Li W, Zhou X, Li Y, *et al*. CircRNA-CREIT inhibits stress granule assembly and overcomes doxorubicin resistance in TNBC by destabilizing PKR. Journal of Hematology & Oncology. 2022; 15: 122. https://doi.org/10.1186/s13045-022-01345-w.

[36] Tong F, Hu H, Xu Y, Zhou Y, Xie R, Lei T, *et al*. Hollow copper sulfide nanoparticles carrying ISRIB for the sensitized photothermal therapy of breast cancer and brain metastases through inhibiting stress granule formation and reprogramming tumor-associated macrophages. Acta Pharmaceutica Sinica. B. 2023; 13: 3471–3488. https://doi.org/10.1016/j.apsb.2022.11.003.